

5-2009

## Turn Constrained Path Planning Problems

Victor M. Roman  
*University of Nevada, Las Vegas*

Follow this and additional works at: <https://digitalscholarship.unlv.edu/thesesdissertations>



Part of the [Navigation, Guidance, Control and Dynamics Commons](#), [Other Computer Sciences Commons](#), and the [Theory and Algorithms Commons](#)

---

### Repository Citation

Roman, Victor M., "Turn Constrained Path Planning Problems" (2009). *UNLV Theses, Dissertations, Professional Papers, and Capstones*. 1202.  
<https://digitalscholarship.unlv.edu/thesesdissertations/1202>

This Thesis is protected by copyright and/or related rights. It has been brought to you by Digital Scholarship@UNLV with permission from the rights-holder(s). You are free to use this Thesis in any way that is permitted by the copyright and related rights legislation that applies to your use. For other uses you need to obtain permission from the rights-holder(s) directly, unless additional rights are indicated by a Creative Commons license in the record and/or on the work itself.

This Thesis has been accepted for inclusion in UNLV Theses, Dissertations, Professional Papers, and Capstones by an authorized administrator of Digital Scholarship@UNLV. For more information, please contact [digitalscholarship@unlv.edu](mailto:digitalscholarship@unlv.edu).

TURN CONSTRAINED PATH PLANNING PROBLEMS

by

Victor M. Roman

Bachelors of Science in Electronic Engineering  
Northrop University  
1984

Bachelor of Science in Computer Science  
University of Nevada, Las Vegas  
2006

A thesis submitted in partial fulfillment  
of the requirement for the

Master of Science Degree in Computer Science  
Computer Science Department  
School of Computer Science

Graduate College  
University of Nevada, Las Vegas  
May 2009

UMI Number: 1472438

### INFORMATION TO USERS

The quality of this reproduction is dependent upon the quality of the copy submitted. Broken or indistinct print, colored or poor quality illustrations and photographs, print bleed-through, substandard margins, and improper alignment can adversely affect reproduction.

In the unlikely event that the author did not send a complete manuscript and there are missing pages, these will be noted. Also, if unauthorized copyright material had to be removed, a note will indicate the deletion.

UMI<sup>®</sup>

---

UMI Microform 1472438  
Copyright 2009 by ProQuest LLC  
All rights reserved. This microform edition is protected against  
unauthorized copying under Title 17, United States Code.

---

ProQuest LLC  
789 East Eisenhower Parkway  
P.O. Box 1346  
Ann Arbor, MI 48106-1346



**Thesis Approval**  
The Graduate College  
University of Nevada, Las Vegas

APRIL 13TH, 2009

The Thesis prepared by

VICTOR M. ROMAN

Entitled

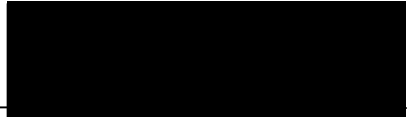
TURN CONSTRAINED PATH PLANNING PROBLEMS

is approved in partial fulfillment of the requirements for the degree of

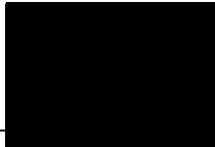
MASTER OF SCIENCE IN COMPUTER SCIENCE



*Examination Committee Chair*



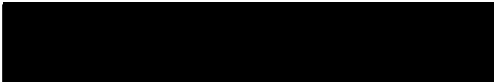
*Dean of the Graduate College*



*Examination Committee Member*



*Examination Committee Member*



*Graduate College Faculty Representative*

## ABSTRACT

### Turn Constrained Path Planning Problems

by

Victor M. Roman

Dr. Laxmi Gewali, Examination Committee Chair  
Professor of Computer Science  
University of Nevada, Las Vegas

We consider the problem of constructing multiple disjoint paths connecting a source point  $s$  to a target point  $t$  in a geometric graph. We require that the paths do not have any sharp turn angles. We present a review of turn constrained path planning algorithms and also algorithms for constructing disjoint paths. We then combine these techniques and present an  $O(n \log n)$  time algorithm for constructing a pair of edge disjoint turn constrained paths connecting two nodes in a planar geometric graph. We also consider the development of a turn constrained shortest path map in the presence of polygonal obstacles. Prototype implementations of the proposed algorithms are also presented. These problems have application for trajectory planning for unmanned aerial vehicles (UAV).

## TABLE OF CONTENTS

ABSTRACT . . . . .	iii
LIST OF FIGURES . . . . .	vi
LIST OF TABLES . . . . .	viii
ACKNOWLEDGMENTS . . . . .	ix
CHAPTER 1 INTRODUCTION . . . . .	1
CHAPTER 2 TURN CONSTRAINED DISJOINT PATHS . . . . .	3
2.1 Turn Constrained Shortest Path . . . . .	3
2.2 Shortest Disjoint Path Pairs . . . . .	5
2.3 Constrained Disjoint Path Pairs . . . . .	8
CHAPTER 3 CONSTRAINT SHORTEST PATH MAP (CSPM) . . . . .	13
3.1 Shortest Path Map . . . . .	13
3.2 Constrained Shortest Path Map . . . . .	22
3.3 Extending CSPM to add partially forbidden region . . . . .	25
CHAPTER 4 IMPLEMENTATION . . . . .	27
4.1 Turn Constrained Disjoint Path Interface . . . . .	27
4.1.1 Interface Description . . . . .	27
4.1.2 Icon Functionality Description . . . . .	28
4.1.3 Program menu items . . . . .	29
4.1.4 Visibility Edge Generation . . . . .	30
4.1.5 Constrained Path Generation . . . . .	31
4.2 Constrained Shortest Path Map Interface . . . . .	31
4.2.1 Interface Description . . . . .	32
4.2.2 Icon Functionality Description . . . . .	34

4.2.3	Program Submenu Description . . . . .	36
4.2.4	SPM Implementation . . . . .	38
CHAPTER 5	CONCLUSION . . . . .	41
BIBLIOGRAPHY	. . . . .	43
VITA	. . . . .	45

## LIST OF FIGURES

Figure 2.1	Transform $G$ to $G'$ . . . . .	4
Figure 2.2	Example Path Types . . . . .	5
Figure 2.3	Shortest Path from $s$ to $t$ . . . . .	6
Figure 2.4	Tagging of Shortest Path . . . . .	7
Figure 2.5	Disjoint Path Pair . . . . .	7
Figure 2.6	Cut Path . . . . .	8
Figure 2.7	Constrained Path $P1$ . . . . .	9
Figure 2.8	Tagging of Constrained Path $P1$ . . . . .	9
Figure 2.9	Constrained Disjoint Path Pair $P1$ and $P2$ . . . . .	10
Figure 3.1	SPM Graph (Single obstacle) . . . . .	13
Figure 3.2	Bisector . . . . .	14
Figure 3.3	SPM Graph (two obstacles) . . . . .	16
Figure 3.4	SPM for many obstacles . . . . .	17
Figure 3.5	$s$ Vertex Free Region . . . . .	18
Figure 3.6	$s$ Vertex Free region with Bisector . . . . .	19
Figure 3.7	$V_i$ Generated Free Region . . . . .	20
Figure 3.8	Illustrating Restricted Faces and Forbidden regions . . . . .	23
Figure 3.9	Final CSPM . . . . .	26
Figure 4.1	Constraint GUI Layout . . . . .	28
Figure 4.2	Constraint Program Main . . . . .	28
Figure 4.3	Program Options . . . . .	30
Figure 4.4	Visibility Edges . . . . .	31
Figure 4.5	Constrained Paths . . . . .	32



Figure 4.6	Planar GUI Layout . . . . .	33
Figure 4.7	Partition GUI Layout . . . . .	33
Figure 4.8	Planar Program Main GUI . . . . .	34
Figure 4.9	Planar Program Partition GUI . . . . .	35
Figure 4.10	Planar Program File Options . . . . .	37
Figure 4.11	Planar Program Partition options . . . . .	38
Figure 4.12	Graph G Before Partition . . . . .	39
Figure 4.13	Graph G Partitioned into regions . . . . .	40
Figure 4.14	Shortest Path from s to t . . . . .	40

## LIST OF TABLES

Table 4.1	Icon description . . . . .	29
Table 4.2	File menu Items description . . . . .	29
Table 4.3	Options menu Items description . . . . .	30
Table 4.4	Icon description . . . . .	35
Table 4.5	Icon description continued . . . . .	36
Table 4.6	File menu Items description . . . . .	36
Table 4.7	Options and Help menu Items description . . . . .	36
Table 4.8	File and Options menu Items description . . . . .	37

## ACKNOWLEDGMENTS

I would like to thank my advisor, Dr. Laxmi Gewali, for his support and guidance during the course of my graduate studies. Dr. Gewali was always available and was extremely generous with his time.

Additional thanks to Professor Lee Mish who believed in me when I first decided to start graduate school, to Dr. Jan Pedersen whom would recognize the influence of his programming style in the implementation phase of this project, as well as Dr. Ajoy K Datta, Dr. John Minor, and Dr. Yoowan Kim.

Finally, I would like to thank my father for his unwavering support and encouragement throughout my years of study.

## CHAPTER 1

### INTRODUCTION

The problem of computing shortest path in a weighted network has attracted the interest of many researchers and several efficient algorithms to solve this problem have been reported [3, 10]. In a two dimensional Euclidian plane that contains obstacles, the application of shortest path is used to determine a collision free path connecting two given points. Note that a path that traverses only the free-space is called a collision-free path. One of the approaches for finding the shortest collision-free path in 2-dimensions is to convert the problem into an equivalent problem in a geometric graph. Specifically, the collection of obstacles in 2-dimensions is converted into a graph called the visibility graph [10]. It has been formally established that the shortest collision-free path can be computed by finding the shortest path in the visibility graph. The main reason behind this fact is that if a shortest path touches the obstacle, then it must touch in one of the vertices. Several variations of shortest-path computations have been considered. One such variation is to find a path connecting two given vertices with a minimum number of link hops. Such a path is called a link minimized path and efficient algorithms for computing such path are reported in [9]. Another variation of shortest-path problem is obtained by imposing turn angle constraint. Specifically, it is required to construct a shortest path in the presence of obstacles such that the turn implied by consecutive segments in the path is no more than a given value. One of the algorithms for computing the turn constrain shortest path in two dimensions was reported by Borujerdi and Uhlmann in [1].

Several researchers have also considered the problem of computing more than one short length path connecting two vertices in a network. One of the early results on computing a pair of node disjoint paths connecting two given vertices in a network was

given in [13].

In this thesis we consider the problem of computing multiple node disjoint shortest path that do not contain a sharp turn angle. In Chapter 2 we present an algorithm for computing a Turn Constrained Disjoint Path Pair in a planar two dimensional geometric network. The algorithm executes in  $O(n \log n)$  time, where  $n$  is the number of vertices in the network. We then extend the algorithm to compute Turn Constrained k-Disjoint Paths running in  $O(kn \log n)$  time. In Chapter 3 we address the problem of constructing a constrained shortest path map (CSPM). It may be noted that the constrained shortest path map is a generalization of the standard shortest path map that is used for constructing shortest paths for a fixed start point  $s$  and several query target point  $t$ . Once the CSPM is available future queries for the shortest constrained path from a source point  $s$  to a target point  $t$  contained in the CSPM will take at most  $O(n)$  time, where  $n$  is the number of vertices in the graph. Chapter 4 presents a description of the prototype programs for the implementation of the proposed algorithms. The actual implementation is done in the Java programming language. Finally in Chapter 5, we discuss the results of the experimental investigation and avenues for future extension of the proposed algorithms.

## CHAPTER 2

### TURN CONSTRAINED DISJOINT PATHS

#### 2.1 Turn Constrained Shortest Path

In this chapter we consider the problem of planning multiple disjoint short length paths connecting a source point  $s$  to a target point  $t$  in a 2-D geometric graph such that the path has no turn angle more than a given value.

Finding a shortest path connecting two vertices in a graph is a well explored problem and several algorithms for obtaining the solution have been reported [3, 4]. A path extracted from a geometric graph consists of a sequence of line segments. Two consecutive line segments in the path define the turn angle between them. In many applications, a path with a sharp turn angle may not be acceptable. For example, sharp turn paths can not be used by aerial vehicles. In fact most aerial vehicles can not make a turn of more than  $30^\circ$  [6]. While a variety of algorithms have been developed for constructing shortest path [3, 4], only a few algorithms have been reported addressing the turn constraint property. One of the important algorithmic results on turn constrained shortest path was developed by Boroujerdi and Uhlmann [1]. The algorithm reported in their paper [1] uses a graph transformation technique to solve the turn constrained shortest path problem in a  $O(|E|\log|V|)$  time. Their technique is to transform a given graph  $G$  into  $G'$  such that the shortest path in  $G'$  corresponds to a turn constrained shortest path in  $G$ . An overview of this technique can be briefly described as follows.

For a given graph  $G(V, E)$ , each edge  $e_i \in E$  become a vertex  $e'_i \in V'$  in the transformed graph  $G'(V', E')$ . Two vertices  $e'_i$  and  $e'_j$  in  $E'$  are connected by an edge  $h_{ij}$  if the corresponding edges  $e_i$  and  $e_j$  in  $G$  are adjacent to each other. The weight of an edge  $h_{ij}$  in  $E'$  is set to the sum of the weights of  $e_i$  and  $e_j$  in  $E$  if the implied angle between  $e_i$  and

$e_j$  is less than or equal to the max turn angle  $\theta_{max}$ . If the implied turn angle between  $e_i$  and  $e_j$  is more than  $\theta_{max}$  then the weight of  $h_{ij}$  is set to infinity.

Figure 2.1 illustrates an example of the original graph and the transformed graph. In the figure, two different paths connecting  $v_1$  to  $v_6$  are shown emphasized. Note that a sharp turn between  $e_7$  and  $e_{10}$  at pivot vertex  $v_5$  in  $G$  is shown as an edge with weight infinity ( $\infty$ ) in  $G'$ . Thus a shortest path between two vertices in  $G'$  correspond to a

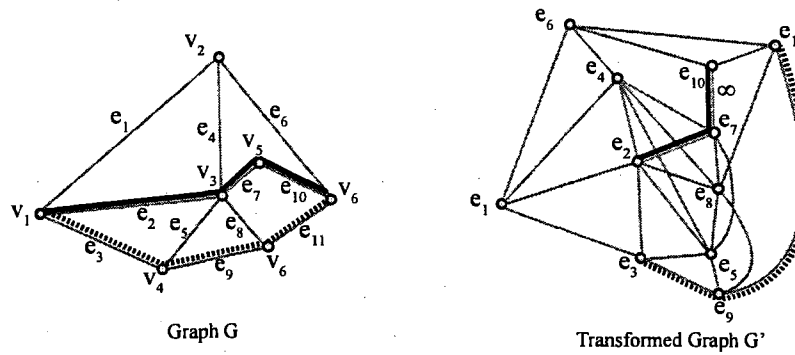


Figure 2.1: Transform  $G$  to  $G'$ .

shortest path without a sharp-turn, ( $\leq \theta_{max}$ ), in  $G$ . The actual path can be computed by applying the standard Dijkstra's shortest path algorithm [4]. It can be observed that the number of edges in the transformed graph  $G'$  can become very high for a dense graph  $G$ . Let  $d_i$  be the degree of the pivot vertex  $v_i$  in  $G$  such that  $v_i \in V$  where  $\{v_i | v_i \text{ is a pivot vertex}\}$ . Then the number of edges in  $G'$  corresponding to  $v_i$  is  $\binom{d_i}{2}$ . Hence the total number of edges in  $G'$  is:

$$|E| = \sum_{i=1}^{|V|} \binom{d_i}{2} \dots \dots \dots (2.1)$$

Boroujerdi and Uhlmann [1] describe the transformation process for the purpose of explaining the algorithm. For actual implementation the graph transformation need not be explicitly done. While applying Dijkstra's shortest path algorithm in  $G$ , the implied sharp turn angle between consecutive edges can be checked on the fly. The turn constrained algorithm reported in [1] runs in time  $O(|E| \log |V|)$ .

## 2.2 Shortest Disjoint Path Pairs

In the context of planning multiple paths connecting a start node  $s$  to a target node  $t$ , the notion of **disjoint-path** becomes useful. A pair of paths are called **node disjoint** if they do not share nodes. If a pair of paths are not allowed to share edges then they are called **edge disjoint**. Note that node disjoint paths are also edge disjoint paths. Since we are interested in studying disjoint paths connecting two given nodes, start node  $s$  and target node  $t$ , we require the paths to share both  $s$  and  $t$ . The disjoint paths connecting  $s$  and  $t$  can be formally defined as follows.

**Definition 2.1** *Given a graph  $G$ , a source node  $s$ , and a target node  $t$ , then a pair of paths connecting  $s$  and  $t$  is called **node disjoint** if the paths do not share any node in their interior.*

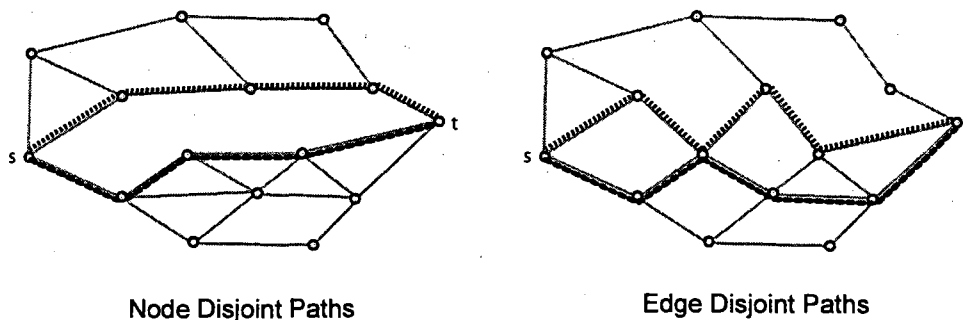


Figure 2.2: Paths Types.

Figure 2.2 illustrates a pair of disjoint paths connecting  $s$  and  $t$ . The path-pair shown in the left is node disjoint while the pair on the right side of the figure are just edge-disjoint. The problem of computing shortest pair of  $s$ - $t$ -disjoint paths was first considered by Suurballe and Tarjan [13]. They reported an  $O(m \log_{(1+m/n)} n)$  algorithm for solving the problem, where  $m$  and  $n$  are the number of edges and the number of vertices respectively in the graph. Their technique is to convert the graph into a directed graph that satisfies the anti-symmetric property. Note that a graph is said to satisfy



the anti-symmetric property if the presence of an edge  $(u, v)$  implies that an edge  $(v, u)$  is not present. The algorithm uses complicated data structures which are difficult to implement. Recently, a very simple algorithm to compute a pair of short length node-disjoint paths connecting two vertices in a geometric network was reported in [8]. The algorithm runs in  $O(n^2)$  time and is very simple to implement. This algorithm uses a **path-tagging** technique for the construction of a path pair in a graph  $G$ . Since we will be using this technique for developing an algorithm for turn constrained path pair we briefly describe it below.

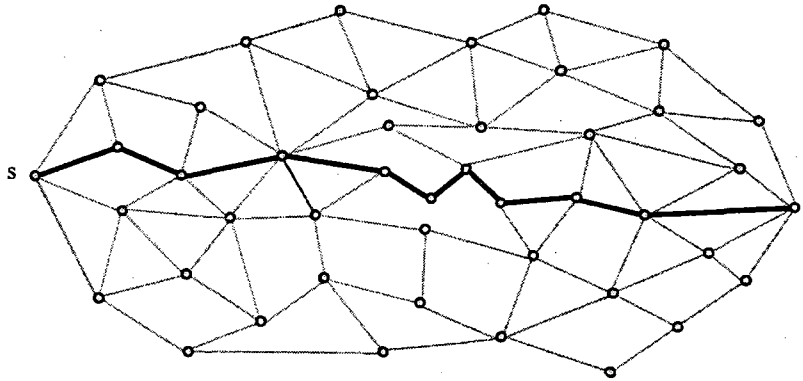


Figure 2.3: Shortest Path from  $s$  to  $t$ .

Consider a shortest path connecting  $s$  and  $t$  in a 2-d network as shown in Figure 2.3. The shortest path is shown highlighted with thick edges. Now consider the set of edges incident on the shortest path except those on  $s$  and  $t$ . We call these edges **sleeve-edges**. The sleeve edges are drawn dashed in Figure 2.4. The process of directing sleeve edges away from the path is called **path-tagging**. Let  $G^1$  denote the network obtained by path tagging the shortest  $s$ - $t$ -path  $p_1$  in a geometric graph  $G$ . If we compute a shortest  $s$ - $t$ -path  $p_2$  in  $G^1$  we find that  $p_1$  and  $p_2$  are node disjoint; the computed path  $p_2$  is shown in Figure 2.5. However in some situations this technique of straight forward path tagging may fail to work. This happens when the shortest  $s$ - $t$ -path becomes a **cut-path**. A  $s$ - $t$ -path  $P$  is

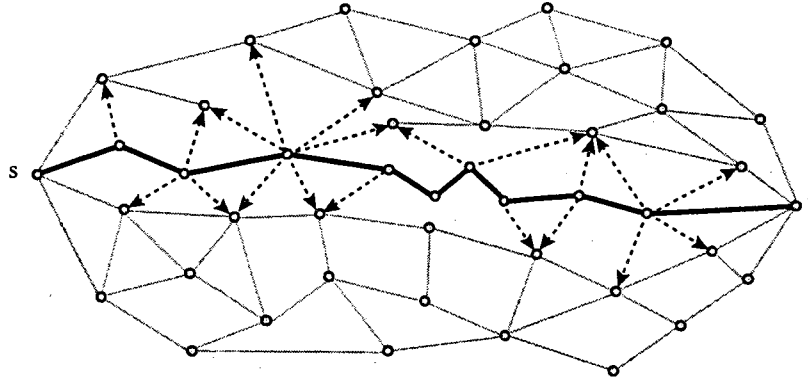


Figure 2.4: Tagging of Shortest Path.

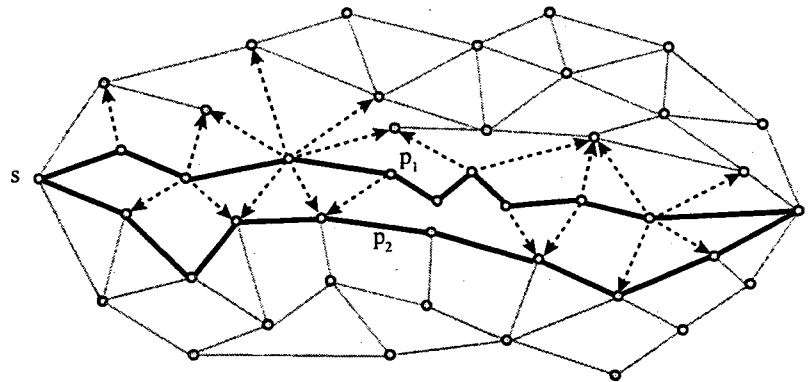


Figure 2.5: Disjoint Path Pair.

called a cut-path if a sub path of  $P$ , not containing  $s$  and  $t$  partitions the network into two disjoint components. Figure 2.6 shows a network in which the shortest  $s$ - $t$ -path is a cut path. From Figure 2.6, it is clear that when the shortest  $s$ - $t$ -path  $P_1$  is a cut path it is not possible to use it as a candidate for short length disjoint path-pair. A different kind of path tagging should be used in such cases and the detail algorithm is reported in [8].

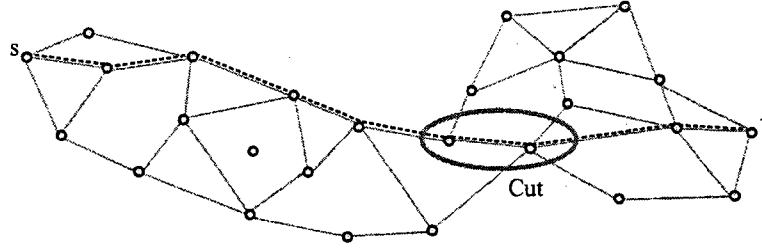


Figure 2.6: Illustration of cut-path formation.

### 2.3 Constrained Disjoint Path Pairs

We are interested in the development of an efficient algorithm for constructing multiple ( $k$ ) node disjoint short length paths connecting two nodes in a geometric graph such that the paths do not contain sharp turns. In particular, we start with the development of an efficient algorithm for constructing a pair of ( $k = 2$ ) node disjoint paths without sharp turns. We combine the techniques for constructing the angle constrained shortest path and node disjoint paths, briefly reviewed in the previous two sections, to solve the problem which can be formally stated as follows.

#### Constrained Disjoint Path-Pair Problem (CDPP)

**Given:** A planar geometric graph  $G(V, E)$ , start node  $s$ , target node  $t$  and maximum turn angle  $\theta_{max}$ .

**Question:** Construct a short-length node disjoint path-pair  $p_1$  and  $p_2$  connecting  $s$  to  $t$  such that the paths are of short lengths and do not contain a turn angle greater than  $\theta_{max}$ .

To make sure that the path-pair do not have a turn angle greater than  $\theta_{max}$  we use the graph transformation method formulated by Boroujerdi and Uhlmann [1]. Furthermore, to make sure that the pair are disjoint in their interior and are of short length, we use the path-tagging technique presented in [8]. The approach is first to find the turn constrained shortest path  $P$  connecting  $s$  to  $t$ . We then check whether  $P$  is a cut-path or not for

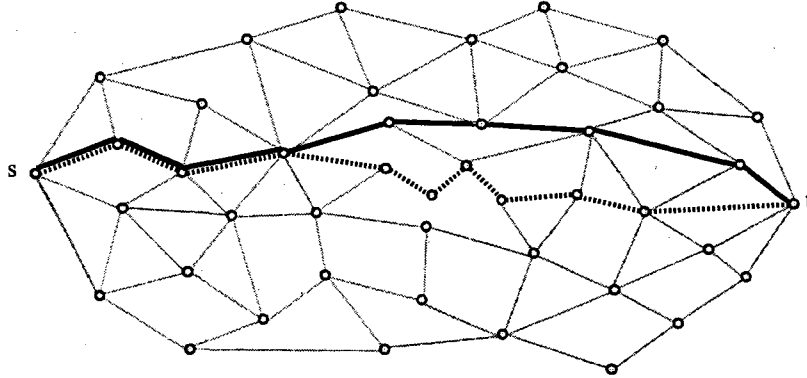


Figure 2.7: Constrained Path  $p_1$ .

the given geometric graph. Figure 2.7 shows the shortest path from  $s$  to  $t$ , represented by a sequence of dashed edges. This path has a sharp turn that violates the constrain property. We use the graph transformation method from [1] implicitly in the graph and apply Dijkstra's shortest path algorithm to obtain the shortest  $s$ - $t$ -path  $p_1$  that does not have turn angle greater than  $\theta_{max}$ . This turn-constrained shortest path  $p_1$  is tagged by directing edges incident on the path away from it, edges incident at  $s$  and  $t$  are not tagged. The weight of the edges of path  $p_1$  are set to infinity. Let the resulting graph (after path tagging and infinity weight assignment) be  $G'$ , Figure 2.8. We then compute

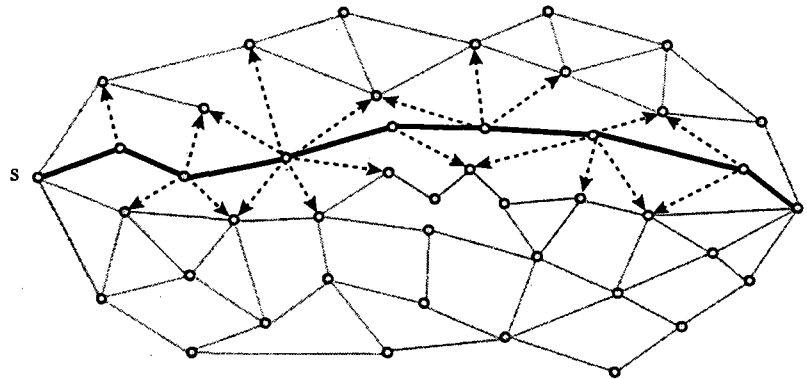


Figure 2.8: Tagging of Constrained Path  $p_1$ .

the turn constrained shortest path  $p_2$  between  $s$  and  $t$  in  $G'$ . The path  $p_2$  is edge disjoint due to the path tagging. The pair of paths  $p_1$  and  $p_2$  give the short length disjoint path pair between  $s$  and  $t$ . (If  $p_1$  is a cut path then the boundary of the graph is tagged by following the approach given in [8]). Figure 2.9 shows the final short length disjoint path pair. A sketch of the Turn Constrained Disjoint Path Pair algorithm is shown below.

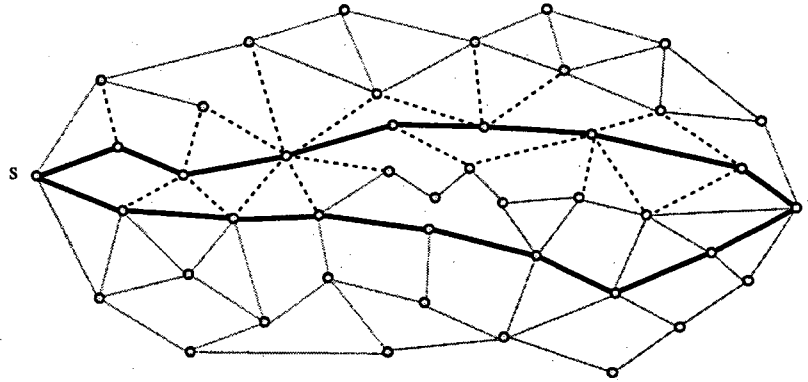


Figure 2.9: Constrained Disjoint Path Pair  $p_1$  and  $p_2$ .

### Turn Constrained Disjoint Path Pairs Algorithm (TCDPP)

- Input:** Geometric planar graph  $G(V, E)$ , start vertex  $s$ , target vertex  $t$ , and angle  $\theta$
- Output:** Turn constrained disjoint pair of paths connecting  $s$  and  $t$
- Step 1:** Create an adjacency list for all consecutive vertices  $v_i, v_j, v_k$  that violate the angle constrain.
- Step 2:** Find the shortest path  $p_1$  from  $s$  to  $t$  in  $G$  for transitions that do not violate the angle constrain.
- Step 3:** If  $p_1$  is a cut path
- Assign counterclockwise direction to the boundary edge from  $s$  to  $t$
  - Perform Path Tagging on the path from  $s$  to  $t$  to obtain graph  $G_1$
  - Find the shortest path  $p_i$  from  $s$  to  $t$  in  $G_1$  for consecutive vertices  $v_i, v_j, v_k$  that do not violate the angle constrain.
  - Replace  $p_1$  by  $p_i$
- endif
- Step 4:** //Find the companion Path  $p_2$
- Perform path tagging to  $p_1$  in  $G$  to obtain  $G_2$
  - Find the shortest path  $p_2$  from  $s$  to  $t$  in  $G_2$  for consecutive vertices  $v_i, v_j, v_k$  that do not violate the angle constrain.
- Step 5:** The output is given by  $p_1$  and  $p_2$

**Theorem 2.1** *The TCDPP algorithm can be executed in  $O(n \log n)$  time.*

**Proof:** By using the implementation technique in [1] Step 1 and Step 2 can be done in  $O(|E| \log |V|)$ . Whether or not a path is a cut path can be done in  $O(|E| \log n)$  time by using point location algorithm from computational geometry [10]. Hence Step 3 takes  $O(|E| \log n)$  time. Since the network is available in doubly connected edge list form, the path tagging can be done in  $O(|E|)$  time. The companion shortest path  $p_2$  can be found in  $O(|E| \log n)$ . Hence Step 4 takes  $O(|E| \log n)$ . This implies that the total time of the entire algorithm is  $O(|E| \log n)$ . Since the network is planar,  $|E| = O(n)$ . Hence the total time is  $O(n \log n)$ .  $\square$

The above algorithm can be extended to generate a set of  $k$  disjoint path by modifying

it so we can make multiple calls to step 4 and find additional companion paths. The modified algorithm is shown below

**Turn Constrained k-Disjoint Path Algorithm (k-TCDP)**

**Input:** Geometric planar graph  $G(V, E)$ , start vertex  $s$ , target vertex  $t$ , angle  $\theta$ , and  $k$  number of disjoint paths desired.

**Output:** Turn Constrained disjoint paths connecting  $s$  and  $t$

**Step 1:** Create an adjacency list for all consecutive vertices  $v_i, v_j, v_k$  that violate the angle constrain.

**Step 2:** Find shortest path  $p_i$  where  $i = 1$ , from  $s$  to  $t$  in  $G_i$  for transitions that do not violate the angle constrain.

**Step 3:** If  $p_i$  is a cut path

a. Assign counterclockwise direction to the boundary edge from  $s$  to  $t$

b. Perform Path Tagging on the path from  $s$  to  $t$  to obtain graph  $G_x$

c. Find the shortest path  $p_x$  from  $s$  to  $t$  in  $G_x$  for consecutive vertices  $v_i, v_j, v_k$  that do not violate the angle constrain

d. Replace  $p_i$  by  $p_x$

endif

**Step 4:** //Find the companion disjoint path

While( $i$  is less than the desire path number and a companion path exists) do

a. Perform path tagging to  $p_i$  in  $G$  to obtain  $G_{i+1}$

b. Find the shortest path  $p_{i+1}$  from  $s$  to  $t$  in  $G_{i+1}$  for consecutive vertices  $v_i, v_j, v_k$  that do not violate the angle constrain

c. Increment  $i$  by one

enddo

**Step 5:** The output is given by  $p_i$

It is straight forward to conclude that the k-TCDP algorithm executes in  $O(k|E| \log n)$  time.

## CHAPTER 3

### CONSTRAINT SHORTEST PATH MAP (CSPM)

#### 3.1 Shortest Path Map (SPM)

Consider a collection of convex obstacles  $Q_1, Q_2, \dots, Q_k$  in two dimensions. For computing collision-free shortest path from start points  $s$  to any other goal points  $g_1, g_2, \dots, g_m$ , the notion of the shortest path map (SPM) has been used very successfully [7, 11]. Broadly speaking, the shortest path map induced by a collection of obstacles and a source point  $s$  is the partitioning of the free space (space without obstacles) into regions such that the shortest path from  $s$  to any point in a region passes through the same set of obstacle vertices. We can elaborate the formation of SPM with some examples as follows.

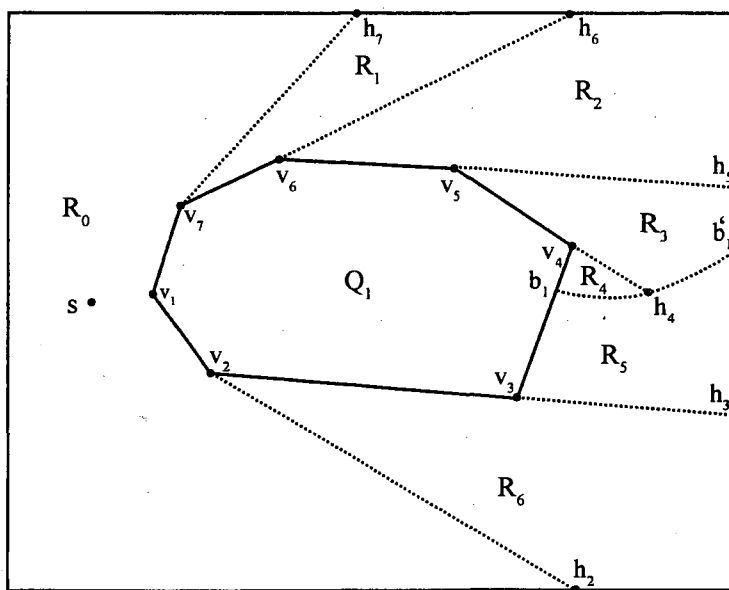


Figure 3.1: SPM Graph (Single obstacle).



First consider only one obstacle  $Q_1$  and a source point  $s$  enclosed in a rectangular box as shown in Figure 3.1 (drawn by solid line segments). Let the list of vertices of obstacle  $Q_1$  be  $v_1, v_2, \dots, v_n$ , when the boundary is traversed in the counterclockwise direction. Consider two **supporting rays** emanating from  $s$  and supporting  $Q_1$  at vertices  $v_i$  and  $v_j$ . Such vertices are called **support-vertices**. Let  $h_i$  and  $h_j$  be the points of intersection (**hit-points**) of the supporting rays with the enclosing rectangular box. The line segment  $(v_i, h_i)$  on the supporting rays is referred to as a **connecting-segment**, shown in Figure 3.1 as dashed segments.

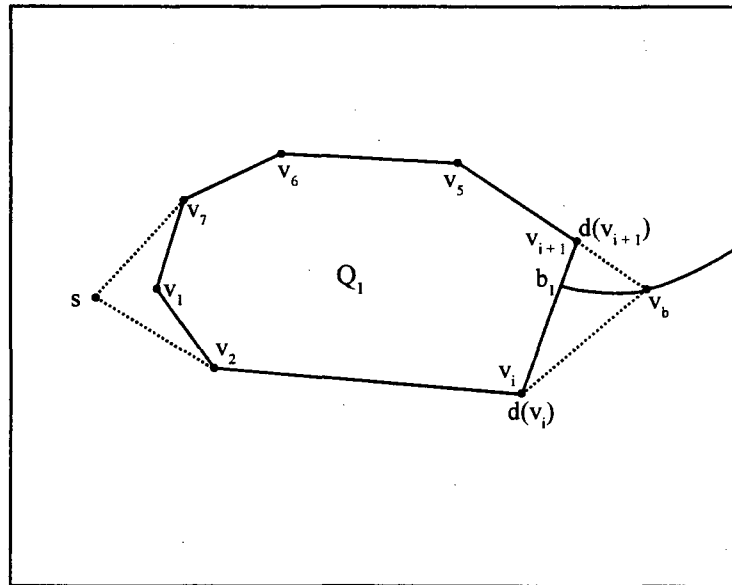


Figure 3.2: Bisector.

The boundary edges of  $Q_1$  can be distinguished into two kinds: (i) Those that are visible from the source point  $s$  are the **visible-edges**, and (ii) the ones that are not visible are the **invisible-edges**. The point  $b_1$  on the boundary of  $Q_1$  for which there are exactly two shortest paths from  $s$ , one each on either side of  $Q_1$ , is called the **bisector point**. It is observed that the bisector point lies on an invisible edge. The invisible edge containing the bisector point is referred to as the **far-edge**.

The locus of the points which are equidistant from  $s$  form a branch of a hyperbola [7] as shown in Figure 3.2. Let  $v_i$  and  $v_{i+1}$  be the vertices that define the far edge, then  $d(v_i)$  will be the shortest counterclockwise distance from  $s$  to  $v_i$  and  $d(v_{i+1})$  will be the shortest clockwise distance from  $s$  to  $v_{i+1}$ . If  $v_b$  is a point on the hyperbola branch, then let  $length(v_i, v_b)$  be the length of the segment  $(v_i, v_b)$  and  $length(v_{i+1}, v_b)$  be the length of the segment  $(v_{i+1}, v_b)$ , thus  $d(v_i) + length(v_i, v_b) = d(v_{i+1}) + length(v_{i+1}, v_b)$  and  $length(v_{i+1}, v_b) - length(v_i, v_b) = d(v_i) - d(v_{i+1})$  where  $v_i$  and  $v_{i+1}$  are the foci of the hyperbola and  $v_b$  belongs to one of the two branches of the hyperbola. If  $d(v_i) > d(v_{i+1})$ , then  $v_b$  belongs to the branch closest to  $v_i$ , otherwise it belongs to the branch closest to  $v_{i+1}$  [7]

If we traverse the boundary of  $Q_1$  in a counterclockwise direction, starting from the vertex closest to  $s$ , the invisible edges encountered before reaching the far-edge are termed as **group-1 invisible edges**. The other invisible-edges that are encountered after the far-edge are termed as **group-2 invisible edges**.

Connecting-segments can be defined for invisible edges other than the far edge. For an invisible edge  $(v_i, v_{i+1})$  in group-1, the corresponding connecting-segment  $(v_{i+1}, h_{i+1})$  is formed by considering the ray  $\overrightarrow{(v_i, v_{i+1})}$ . On the other hand, for an invisible edge  $(v_{i+1}, v_i)$  in group-2, the connecting-segment  $(v_i, h_i)$  is formed by considering ray  $\overrightarrow{(v_{i+1}, v_i)}$ . It is noted that the hit point  $h_i$  for constructing the connecting segments for the invisible edges could be either on the enclosing rectangle or on the bisector parabola.

The set of connecting segments and hyperbola branches partition the free space into  $q$  regions  $R_0, R_1, R_2, \dots, R_q$ , where  $q$  is the total number of connecting segments. Corresponding to each connecting segment  $(v_i, h_i)$  there is a unique free-region. A connecting segment will partition a region in at most two new smaller regions if and only if both  $v_i$  and  $h_i$  are on the boundary of the original region, otherwise the connecting segment will join the obstacle boundary with the region boundary.

**Definition 3.1** *The collection of free-regions formed by the set of connecting segments and bisector hyperbola branches is called the Shortest-Path Map (SPM) for source point*

s. Figure 3.1 shows the shortest path map for one convex obstacle, where there are seven free regions.

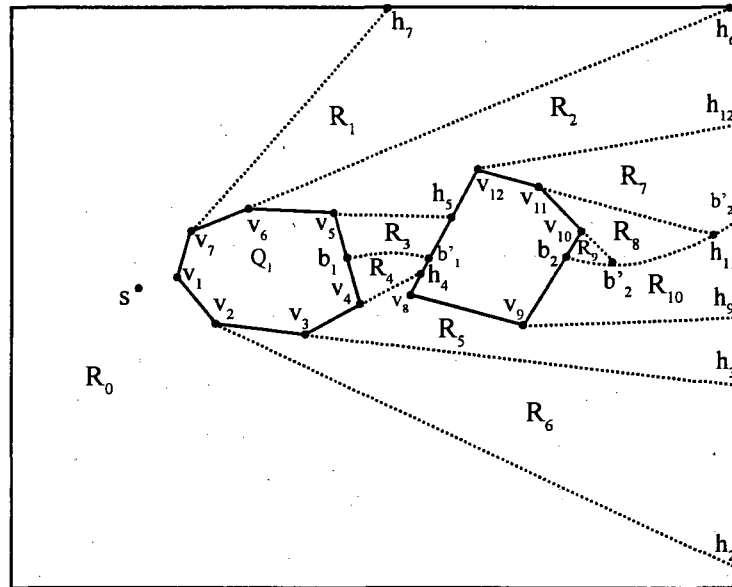


Figure 3.3: SPM Graph (two obstacles).

For more than one obstacle, the corresponding shortest path map can be defined similarly. Support vertices are again defined by considering support rays. The support rays can hit either the boundary of the enclosing rectangle, the boundary of another obstacle or the bisector hyperbola branch. We also need to construct possible connecting edges by considering the connecting-segments incident to a vertex  $v_i$  as secondary source vertices. The shortest path map for two obstacles is shown in Figure 3.3, where there are 10 secondary source points and 11 free regions. Figure 3.4 shows the shortest path map for many obstacles. The shortest path map satisfies several interesting properties which can be summarized as follows

**Property 3.1** *There is exactly one bisector hyperbola branch for each convex obstacle.*

**Property 3.2** *The shortest path from the primary source point  $s$  to any point in a particular region  $R_j$ , of the shortest path map, traverses through the same sequence of secondary*

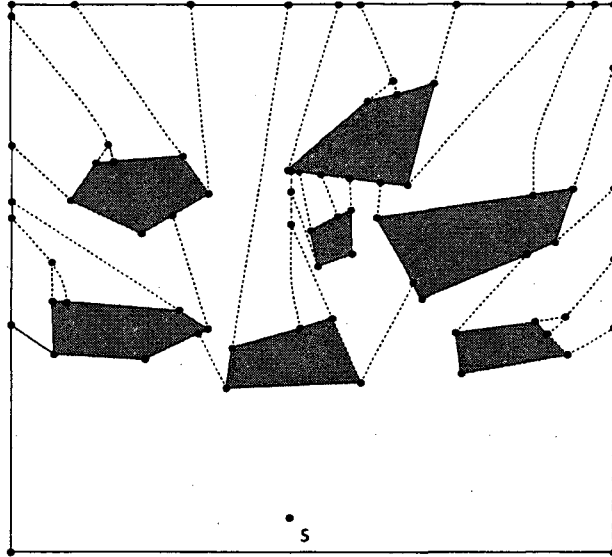


Figure 3.4: SPM for many obstacles.

*source points. Consequently, the shortest paths from  $s$  to all points in a particular region  $R_j$  are identical except for the last segment in the path.*

### Algorithm for Constructing SPM

The basic approach for constructing the SPM was first reported by Lee and Preparata in [7]. Although the algorithm reported in [7] was designed for vertical line segment obstacles, the idea can be carried easily to convex obstacles. Storer and Reif [11] developed an algorithm of time complexity  $O(kn)$  for constructing the SPM, where  $k$  is the number of obstacles and  $n$  is the total number of vertices in all obstacles. The time complexity of this algorithm becomes  $O(n^2)$  when the number of obstacles  $k$  become  $O(n)$ . Finally, an  $O(n \log n)$  time algorithm was presented by Hershberger and Suri [5] that computes the SPM for polygonal obstacles. The algorithm presented in [5] uses complicated tools such as “conformal sub-division” and “artificial wave fronts” that are very difficult for practical implementation. However, this is asymptotically the fastest algorithm for constructing the SPM.

Before we present a simpler algorithm to construct the SPM some definitions are

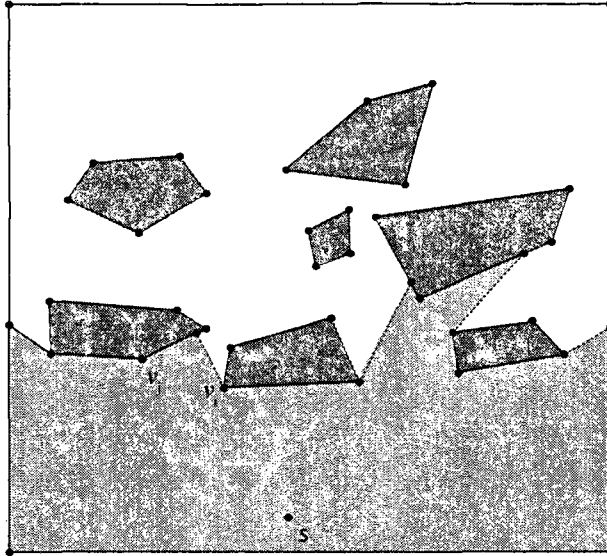


Figure 3.5:  $s$  Vertex Free Region.

useful. A **processed free-region** is the set of points in the free-region for which the shortest path from the source vertex  $s$  is known. Initially, the visibility polygon  $VP(s)$  for the source point  $s$  is taken as the processed free-region. The **front-boundary** of the processed region consists of obstacle edges and connecting edges. The obstacle vertices on the front boundary incident on the connecting edges are precisely the set of **unprocessed vertices**. Figure 3.5 shows the initial processed free-region which is also the visibility polygon  $VP(s)$ .

When the processed free-region is determined, the shortest distance from the source vertex  $s$  to all obstacle vertices is maintained in the record of the corresponding vertex. In the front boundary of the processed free-region, the unprocessed vertex with the least distance from the source vertex  $s$  is referred to as the **closest candidate vertex**. In the Figure 3.5, vertex  $v_i$  is the closest candidate vertex for the indicated processed free region. If an obstacle in the front boundary is supported, then the bisector point can be found and the bisector hyperbola branch can be computed. Figure 3.6 shows the two hyperbola branches for the processed free region.

To expand the processed free-region, the closest candidate vertex  $v_i$  is processed as

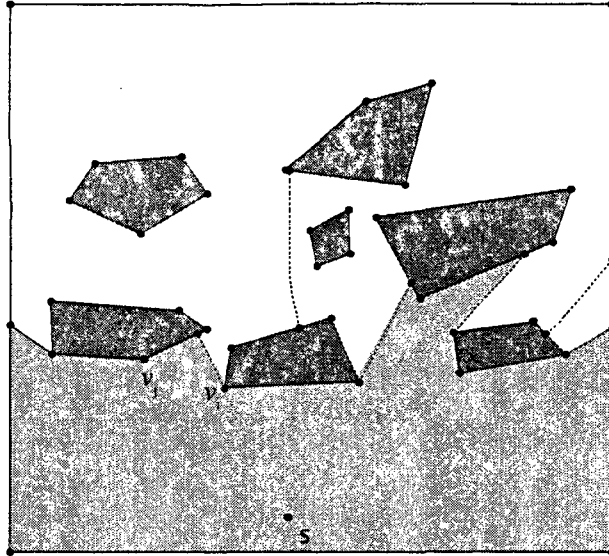


Figure 3.6:  $s$  Vertex Free Region with Bisector.

follows. Let  $OutVP(v_i)$  be the part of the visibility polygon from  $v_i$  that lies outside the currently processed free region  $FR(i-1)$ . The term **out-visibility polygon** is also used to refer to  $OutVP(v_i)$ . In Figure 3.7,  $OutVP(v_i)$  is shown as the region filled with the '+' pattern. After computing the out visibility polygon  $OutVP(v_i)$  the processed free-region  $FR(i-1)$  is expanded by adding  $OutVP(v_i)$  to it and thus obtain  $FR(i)$ . When the out-visibility polygon is added the connecting edges are also included.

This step of updating the processed free-region is continued until all vertices are processed. The final result is the partitioning of the free region which in turn is the shortest path map (SPM) with respect to  $s$ . The processed free-region is maintained in a doubly connected edge list (DCEL) data structure [3] so that the faces of the map can be traversed efficiently.

When a candidate vertex  $v_i$  is processed, new boundary vertices are added to the updated free-region. During the updating task, the shortest distance from the source vertex  $s$  to the new boundary vertices is maintained on the record of the corresponding vertex. If  $d(v_i)$  is the length of the shortest path from  $s$  to  $v_i$ , then the length of the shortest path from  $s$  to a new boundary vertex  $v_b$  is given by  $d(v_b) = d(v_i) + length(v_i, v_b)$ . Note

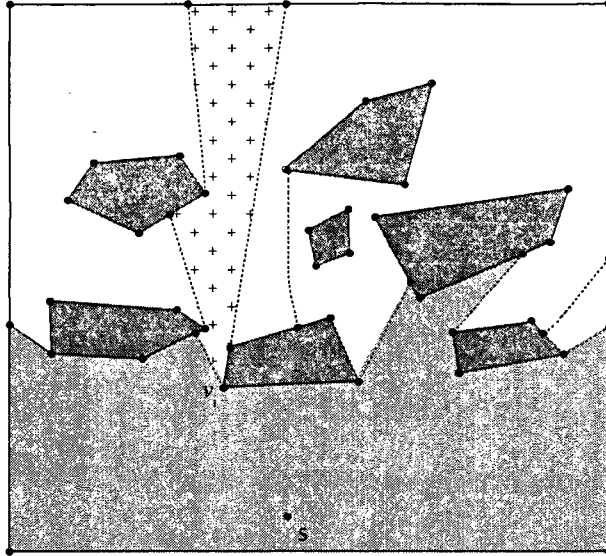


Figure 3.7:  $v_i$  Generated Free Region.

that the line segment connecting  $v_i$  to  $v_b$  lies completely in the free-region. Furthermore, in the structure of  $v_b$ , a reference to the previous vertex in the shortest path from the source vertex  $s$  is recorded. This makes it easy to construct the actual shortest paths.

**Definition 3.2** A vertex  $v$  on the boundary of  $SPM(k)$  is called **Type1** if both boundary edges incident in  $v$  are the edges of the obstacle. In Figure 3.5,  $v_j$  is a **Type1** vertex.

**Definition 3.3** A vertex  $v$  on the boundary of  $SPM(k)$  is called **Type2** if it is an obstacle vertex and a connecting edge is formed by extending an obstacle edge incident at  $v_i$ . In Figure 3.5  $v_i$  is a **Type2** vertex.

**Definition 3.4** An obstacle  $Q$  on the boundary of  $SPM(k)$  is called **boundary supported** if  $Q$  is tangentially supported by two connecting edges.

A formal description of the Algorithm is as follows.

### Visibility Based Algorithm for Shortest Path Map (SPM)

```
Step 1: i.  $k = 0$ 
        ii.  $SPM(k) = \text{visibility polygon } VP(s)$ 
        iii. For all obstacle vertices  $v$  on the boundary of  $VP(s)$  do
            •  $v \cdot dist = length(s, v)$ 
            •  $v \cdot prev = s$ 

//Construct bisectors
Step 2: For boundary supported obstacle  $Q$  do
        • Construct bisector  $b_r$  for  $Q$ 

//Mark processed vertices
Step 3: For all vertices  $v$  on the boundary of  $SPM(k)$  do
        if( $v$  is Type1 or  $v$  is Type2)
             $v \cdot processed = true$ 

Step 4: While all vertices are not processed do
        i. Find the closest candidate vertex  $v_c$  in the  $SPM(k)$ 
        ii. Find  $OutVP(v_c)$ 
        iii.  $SPM(k + 1) = SPM(k) \cup OutVP(v_c)$ 
        iv.  $k = k + 1$ 
        //Construct bisector if any
        v. For all newly formed boundary supported obstacle  $Q$ 
            • Construct bisector  $b_r$  for  $Q$ 
        vi. For all newly formed vertices  $w$  on the boundary of  $SPM(k)$ 
            •  $w \cdot dist = v \cdot dist + length(v, w)$ 
            •  $w \cdot prev = v$ 
        vii. For all vertices  $v$  on the boundary of  $SPM(k)$  do
            • if( $(!v \cdot processed) \ \&\& \ (v \text{ is Type1 or } v \text{ is Type2})$ )
                 $v \cdot processed = true$ 
```

The time complexity of the Visibility Based Shortest Path Map Algorithm can be analyzed in a straightforward manner. The Visibility polygon from a point inside a polygon with holes can be done in  $O(n \log n)$  time [12]. Hence Step 1 can be done in  $O(n \log n)$  time. The visibility polygon can be represented in a DCEL data structure within the same time complexity. Whether or not an obstacle is boundary supported can be determined by checking the angles between the connecting edges and the incident



obstacle edge. Once an obstacle is identified as 'boundary-supported', the corresponding bisector can be determined in time proportional to the number of vertices in the obstacle. Hence Step 2 takes  $O(n)$  time. Whether or not a vertex  $v$  on the boundary of  $SPM(K)$  is Type1 (or Type2) can be done in constant time by checking the edges incident on it. Hence Step 3 take  $O(n)$  time. The closest candidate vertex  $v_c$  can be determined by simply checking the distance to each vertex on the boundary of  $SPM(k)$  which takes  $O(n)$  time.  $OutVP(v_c)$  can be computed in  $O(n \log n)$  time by using a variation of the standard visibility polygon algorithm. The union of  $SPMK$  and  $OutVP(v_c)$  can be done in  $O(n)$  time. Hence Step 4 iii and Step 4 iv can be done in  $O(n)$  time. Similarly each of Step 4 v, Step 4 vi, and Step 4 vii can be done in  $O(n)$  time. The while loop in Step 4 can execute in  $O(n)$  time. Hence total time for Step 4 is  $O(n^2 \log n)$ . This implies that the total time for the entire algorithm is  $O(n^2 \log n)$ .

### 3.2 Constrained Shortest Path Map (CSPM)

The standard shortest path map (SPM) can be used for computing repeated shortest path queries from a fixed source vertex  $s$  to several target vertices. If we want to compute the shortest path between the source vertex  $s$  and a target vertex  $t$  such that the path does not contain sharp turns, then SPM can not be used. We want to construct a constrained shortest path map (CSPM) for a collection of convex polygonal obstacles such that it can be used to compute the shortest path that does not contain sharp turns. The problem can be formally stated as follows

### Constrained Shortest Path Map Problem

**Given:** (i) A collection of convex polygonal obstacles

(ii) Source Vertex  $s$

(iii) Turn angle  $\theta$

**Question:** Construct a constrained shortest path map (CSPM) such that it can be used to find the shortest path between  $s$  and any target point  $t$  such that the path has turns no more than  $\theta$ . The Path can take a turn only at the vertices.

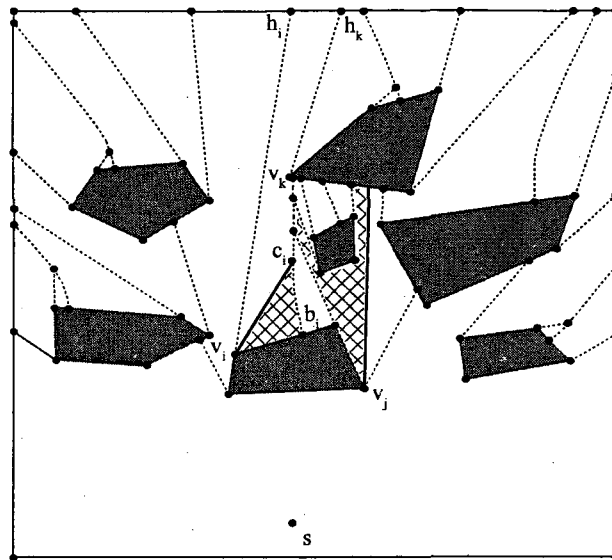


Figure 3.8: Illustrating Restricted Faces and Forbidden regions.

Our approach for constructing the CSPM is to characterize **forbidden regions** in the standard SPM that can not be reached by any path that can turn only on vertices and for which the turn angle is no more than  $\theta$ . Consider a face  $f_i$  rooted at a secondary source vertex  $v_i$ . In Figure 3.8, the region bounded by  $v_i, h_i, h_k, v_k, b_i$  is the face  $f_i$  rooted at  $v_i$ . If the internal angle of  $f_i$  at  $v_i$  is greater than  $\theta$  then not all points inside face  $f_i$  are reachable by a path that turns at  $v_i$ . Such a face which can not be completely reached by the shortest path from the source vertex  $s$  is referred to as a **restricted face**.

A restricted face  $f_i$  can be partitioned into two parts by a **limit chord** of the face. The limiting chord  $v_i c_i$  is such that the angle  $h_i v_i c_i$  is exactly equal to  $\theta$ . The portion of  $f_i$  not reachable by the shortest path with a turn at  $v_i$  greater than  $\theta$ , is called a **forbidden region**, which is shown by a hashed pattern in Figure 3.8. The remaining portion of  $f_i$  is the **reachable region**. The figure also shows the forbidden region corresponding to the restricted face rooted at vertex  $v_j$ . To construct a constrained shortest path map (CSPM) we start from the standard shortest path map (SPM). Each face of the SPM is examined to determine whether or not it is a restricted face. If a face  $f_i$  is restricted then it is partitioned into two parts to identify the corresponding forbidden component. Since the standard SPM is available in a doubly connected edge list form, restricted faces can be easily identified. A restricted face can be processed to extract the forbidden region by constructing the limit chord. The limit chord can be constructed in time proportional to the number of vertices in the restricted face. A formal sketch of the algorithm is listed as the Constrained Shortest Path Map Algorithm.

**Property 3.3** *For points that lie within a forbidden region, no path exist in the CSPM back to  $s$ .*

**Theorem 3.1** *The constrained shortest path map can be constructed in  $O(f_s(n))$  time, where  $n$  is the total number of vertices in the obstacles and  $f_s(n)$  is the time for computing the standard SPM.*

### Constrained Shortest Path Map (CSPM) Algorithm

**Input:** A collection of obstacles, start point  $s$ , maximum turn angle  $\theta$

**Output:** Constrained Shortest Path Map.

**Step 1:** Construct the standard shortest path map (SPM) with source vertex  $s$  and represent it DCEL form.

**Step 2:** Identify and mark all secondary source vertices in the SPM

**Step 3:** For each face in  $f_i$  corresponding to secondary source vertex  $v_i$  do  
If ( $f_i$  is a restricted face)  
partition  $f_i$  by constructing the limiting  $ch_i$

**Step 4:** Output resulting map as CSPM

**Proof:** Step 1 takes  $O(f_s(n))$  time. Once the SPM is available in DCEL data structure, the secondary source vertex of a face can be determined by examining the value of the shortest path distance from  $s$ , (in each face, the vertex with the least distance from  $s$  is the secondary source vertex). Hence Step 2 takes  $O(n)$  time. Whether or not a face  $f_i$  is restricted can be determined by comparing the interior angle of the source vertex with the maximum allowed angle  $\theta$  and this takes constant time. The limiting chord and its use in partitioning the face can be done in time proportional to the number of vertices in the face. Hence Step 3 takes  $O(n)$  time. The total time for the whole algorithm is  $O(f_s(n))$ .  $\square$

### 3.3 Extending CSPM to add partially forbidden region

**Definition 3.5** *In a CSPM, a region partially bounded by bounding rectangle edges, obstacle edges, limit chords and at least one connecting segment is called a **partially forbidden region**.*

**Definition 3.6** *A region in the CSPM containing a point for which there exist a path back to  $s$  in which all turn angles are less than  $\theta$  and it is not the shortest path is called*

*a reachable region*

For any partially forbidden region, at least one of the limit chords connects with a connecting segment. Let us extend the chord until it intersects either an obstacle edge or the enclosing boundary edge. This creates two new regions, a forbidden region and a reachable region. A path exist from all points within the reachable region back to  $s$ . In the final CSPM as shown in Figure 3.9, for points that lie within a free region there exist a shortest path back to  $s$ , for points that lie within a reachable region a path exist back to  $s$  but this path will not be the shortest path.

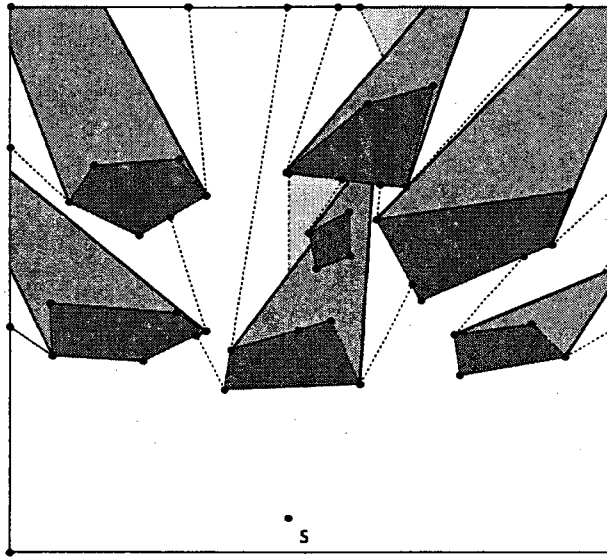


Figure 3.9: Final CSPM.

## CHAPTER 4

### IMPLEMENTATION

This chapter describes an implementation of the two prototype programs used to study the Turn Constrained Disjoint Path and the Constrained Shortest Path Map problems. The programs were implemented in Java, using version 1.4.2

#### 4.1 Constrained Disjoint Path Interface

The implementation of this prototype permits the user to create a network consisting of obstacles which can be edited by adjusting the edges and vertices. Additionally, the source and target points can be changed. Once the network is created the user can initiate the execution of the program to generate the visibility edges and to calculate the shortest disjoint paths from the source vertex  $s$  to a target vertex  $t$ .

##### 4.1.1 Interface Description

The main display window is implemented by extending the JFrame class component in javax.swing. The displayed graphical user interface is made up of several panels, as shown in Figure 4.1. The menu bar panel contains the File and Options menus. All other panes contained within the JFrame object are constructed by using the JPanel class. The left pane contains the buttons used to select and manipulate the network obstacles, vertices, and edges. The center pane contains the main display pane, which is the area where the network is drawn and manipulated. The right pane contains a text line to display the value of the maximum turn-angle as well as a scrollable text area used to display the path information. Finally, the bottom pane contains two buttons used to generate the visibility edges and the shortest constrained paths. Figure 4.2 shows the actual GUI frame as presented to the user.

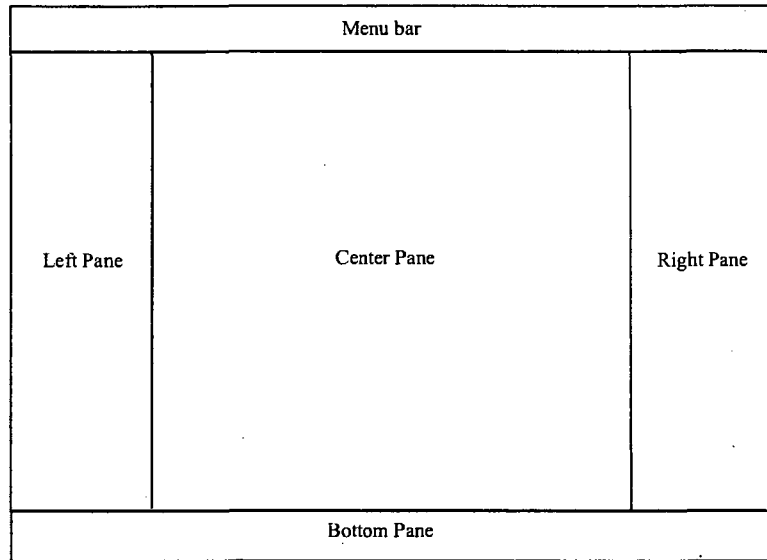


Figure 4.1: Constraint GUI Layout.

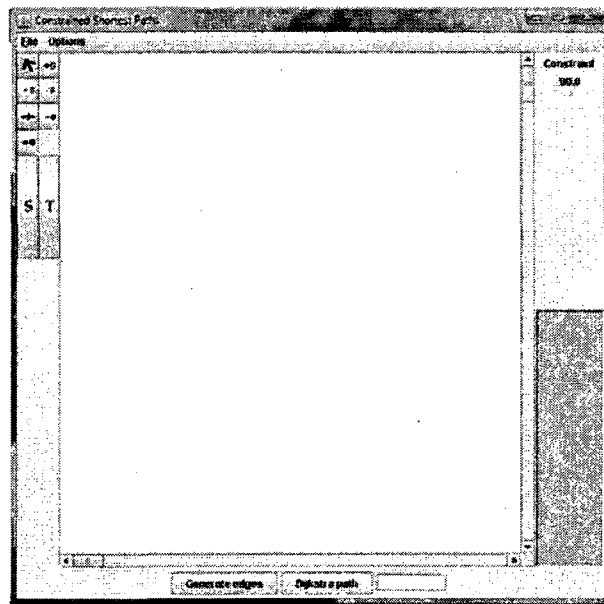


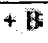






Figure 4.2: Constraint Program Main GUI.

#### 4.1.2 Icon Functionality Description

Table 4.1 describes the functionality of various icons. The first column shows the actual icon and the second column contains a brief description.

Table 4.1: Icon description.

Icon	Description
	Enables the select mode
	If the select mode is enabled, and an obstacle has been selected, the user can change the position of the obstacle by dragging it with the mouse
	Allows the user to add a new obstacle to the graph
	Used for removing the selected obstacle
	Used for splitting an edge of the selected obstacle. The splitting is done by introducing a new vertex
	Used for removing a vertex of the selected obstacle. The vertex closest to the mouse cursor is selected
	Used for updating the coordinates of the closest vertex (from the mouse cursor) of the selected obstacle
S	For Moving the source vertex to a selected mouse cursor position
T	For moving the target vertex to a selected mouse cursor position

#### 4.1.3 Program menu items

The program has two menu items: File and Options. The File menu items enable the user to (i) clear the display screen, (ii) start a new network, (iii) retrieve and open previously saved files, and (iv) save a generated network to a file. A brief description of the File items is provided in Table 4.2. A similar description is provided for the Options items as described in Table 4.3. Figure 4.3 shows the GUI representation of the Options menu items.

Table 4.2: File menu Items description.

File Item	Description
New	Clears the center display panel. Ready for a new network
Open File	Brings up a file selection panel, user can choose an existing graph file
Save File	Brings up a file save panel. The user can save a new file or replace an existing file



Table 4.3: Options menu Items description.

Options Item	Description
Vertex id display	When checked, the vertex id's are displayed
Segment Direction	Used for toggling a direction arrow on the edges
Display Centroid	Used for displaying a dot in the center of the obstacles
Fill Barrier	For displaying obstacles filled with cyan color
Display Angle	When checked the angle made by the incident edges at the vertex is displayed
Single Path	When checked, only one constrained path is displayed; otherwise a pair of constrained paths is displayed

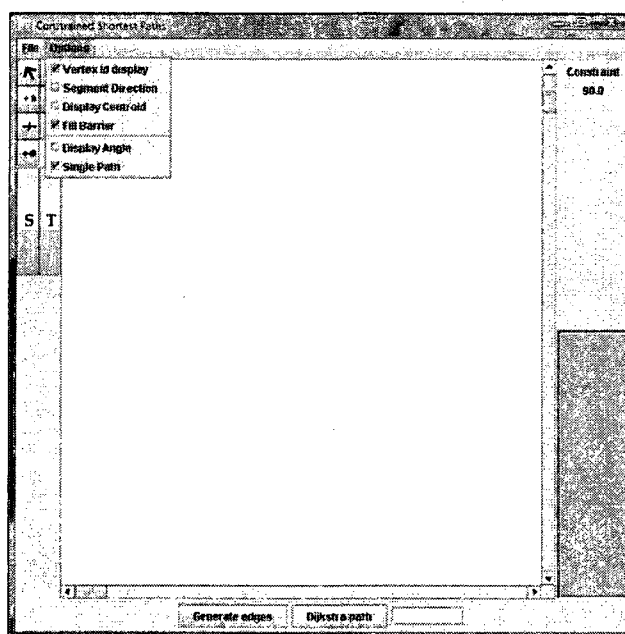


Figure 4.3: Program Options.

#### 4.1.4 Visibility Edge Generation

Once the user has set the coordinates of the source vertex  $s$ , target vertex  $t$ , and has added the obstacles needed to generate the network, the next step is to generate possible paths from  $s$  to  $t$ . The program generates all valid visibility edges between all vertex pairs. Note that no visibility edge may cross an obstacle. The visibility edges are the candidate path edges for the shortest constrained paths from  $s$  to  $t$ . Figure 4.4 shows a network in which the visibility edges have been generated. It is observed that the

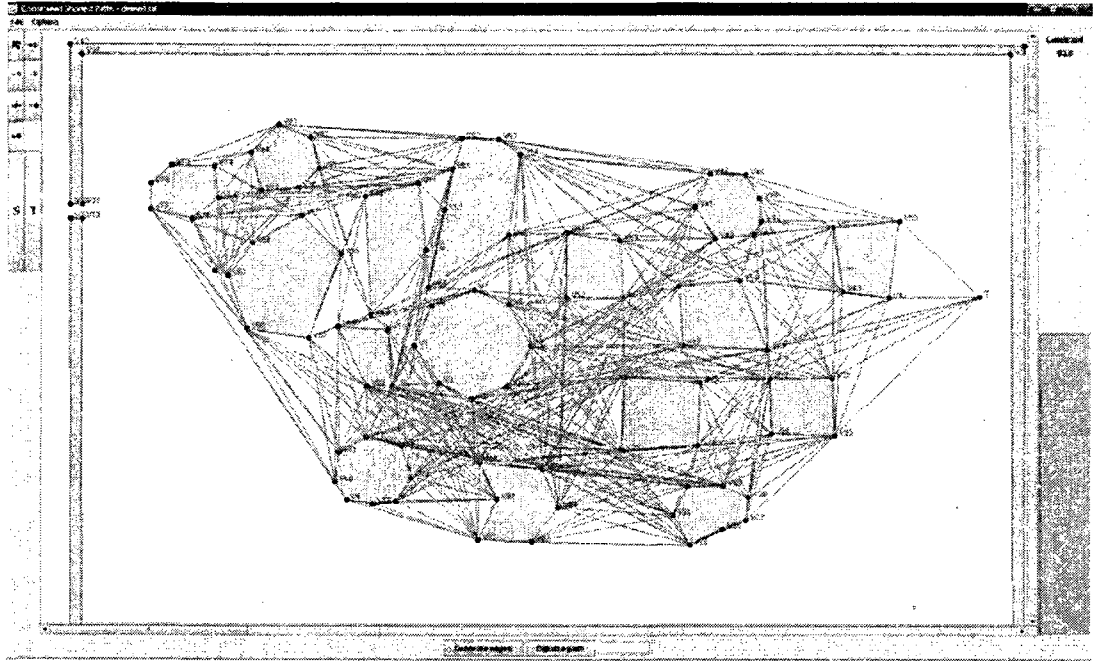


Figure 4.4: Visibility Edges.

generated network need not be planar.

#### 4.1.5 Constrained Path Generation

The final step is to construct the constrained disjoint paths, which is done by applying the algorithm discussed in Chapter 2. The resulting paths are highlighted by the program and the text area on the right side of the pane is updated with the corresponding path information. Depending on the options selected, the program generates either a single angle-constrained path, or a pair of disjoint angle-constrained paths. Figure 4.5 shows a sample output for a pair of short-length disjoint paths.

#### 4.2 Constrained Shortest Path Map Interface

The Constrained Shortest Path Map provides an implementation that allows the user to specify the obstacles and the position of the source point  $s$ . The program partitions the free-space into regions such that the shortest path to any point inside a region goes through the same sequence of vertices. For each vertex, the program stores the magnitude

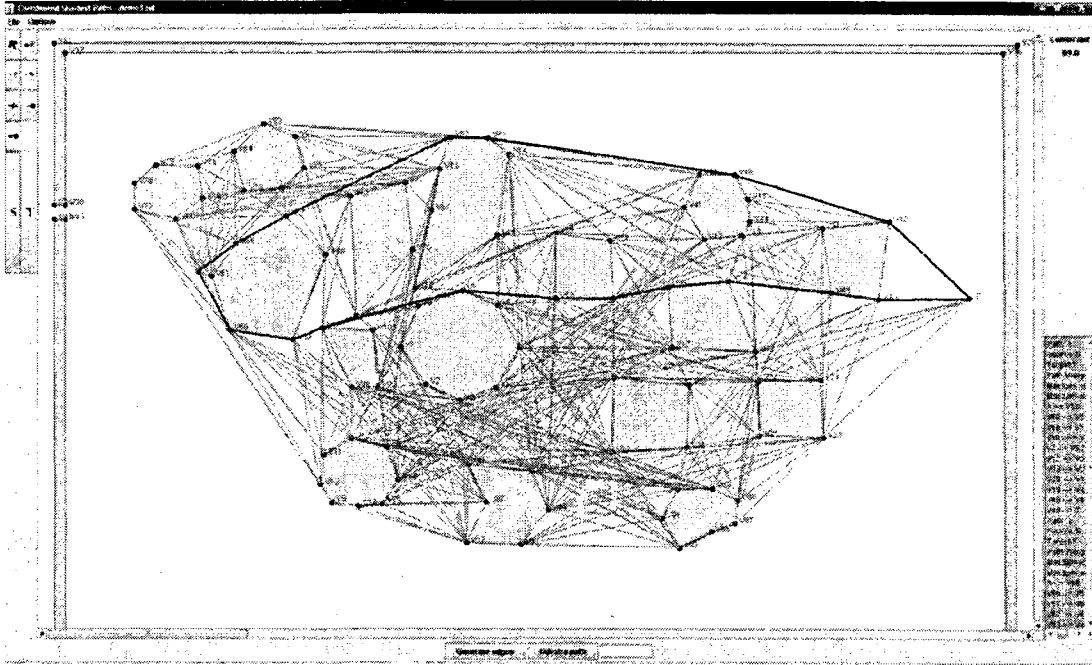


Figure 4.5: Constrained Paths.

of the shortest path from  $s$  and also the record of the previous vertex in the shortest path.

#### 4.2.1 Interface Description

As in the previous program implementation, the main display window is implemented by extending the `JFrame` class component in `javax.swing`. The program has a secondary display window that opens to present the partitioning option. The main display area is used to create and edit the network, while the secondary display window is used to partition the generated network. Once a network is partitioned, it can be saved and reopened in the main window to output the shortest paths for the varying target points  $t$  to the stationary source point  $s$ .

The main GUI is made up of several panels as shown in Figure 4.6. The menu bar contains three selections: File, Options and Help sub-menus. All other panels are within the `JFrame` object and are constructed from `JPanel` class objects. The left pane contains the buttons used to create and edit the network. It is possible to add obstacles and edit their edges and vertices as well as split faces and join obstacles. Not all the buttons

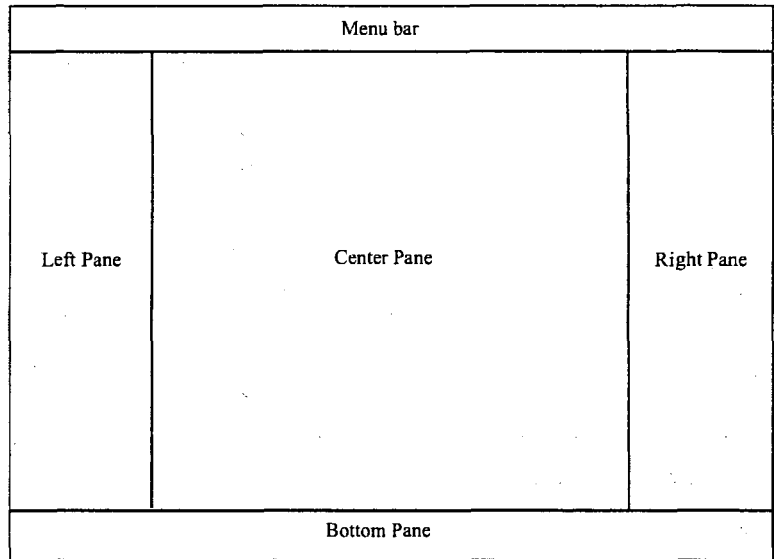


Figure 4.6: Planar GUI Layout.

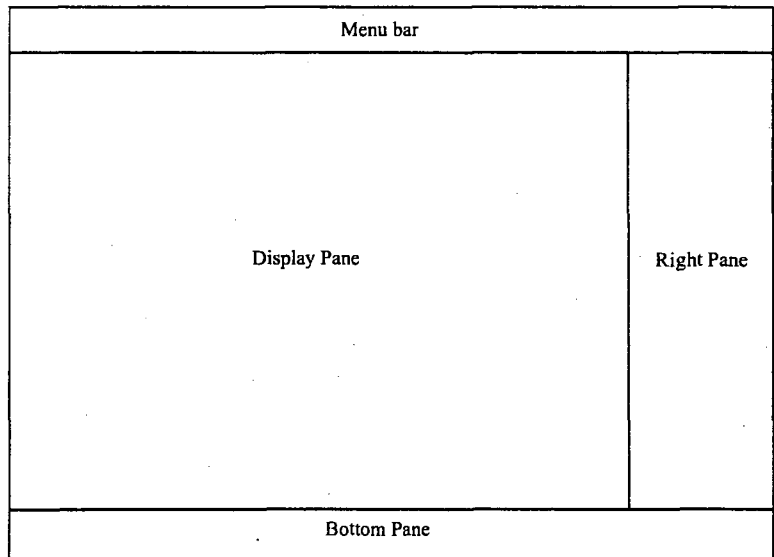


Figure 4.7: Partition GUI Layout.

are functional, buttons that are functional will change color to cyan when selected. The center pane contains the main display pane. This is the area in which the network will be drawn and manipulated. The right pane contains two text boxes: one is used to display the cursor's x-y coordinate as it moves over the center pane and the second one is a large

scrollable text area which is updated with the network information. Finally, the bottom pane contains two buttons: the partition button which will open the secondary window to present the partition GUI, and the Shortest Distance button which will trigger the program to calculate a path from the source vertex to the target vertex for the network that has been previously partitioned.

The secondary display window also contains several panels as shown in Figure 4.7. The menu bar contains the File and Options menus. The center pane is again the main display pane, and the right pane contains a scrollable text area that displays the network information. Finally, the bottom pane contains a single button that initiates the network partition action. Figure 4.8 and Figure 4.9 show the actual GUIs presented to the user by the program.

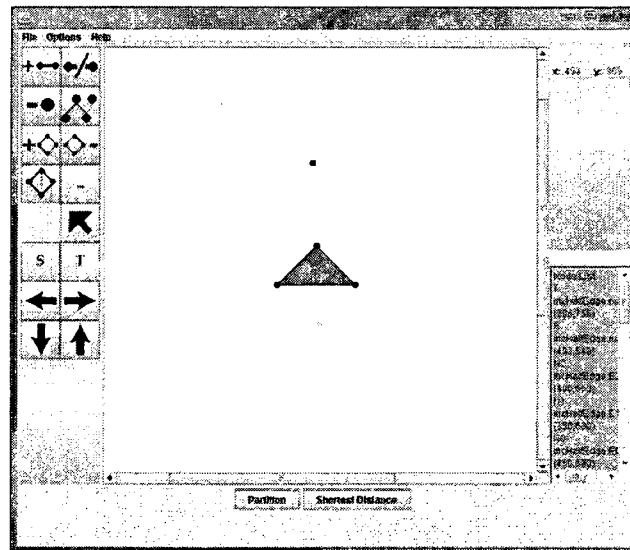


Figure 4.8: Planar Program Main GUI.

#### 4.2.2 Icon Functionality Description

Table 4.4 and Table 4.5 show the description of the icons functionality. The first column shows the image of the icon and the second column gives a brief description of its functionality.

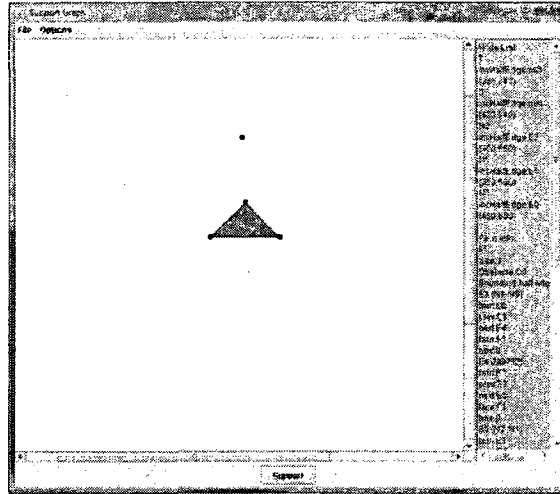


Figure 4.9: Planar Program Partition GUI.

Table 4.4: Icon description.

Icon	Description
	When enabled, the user can add an edge to a selected face. One end of the added edge is the start vertex of the edge closest to the mouse cursor. The other end of the added edge will be the current position of the mouse cursor
	When enabled, the user can split the edge closest to the cursor and add a new vertex to the network
	When enabled, it allows the user to delete the vertex of the selected face which is closest to the cursor position when the left mouse button is pressed
	If the left mouse button is pressed, the closest vertex position to the cursor will be updated to the cursor's x-y coordinates
	After the left mouse button is pressed, the program will add a triangular obstacle to the network. The base of the obstacle will be centered on the cursor's x-y position
	No Functionality Implemented
	When enabled allows the user to split the selected face into two new faces. An obstacle face can not be split

Table 4.5: Icon description continued.






Icon	Description
C	Create a connection between two vertices
	When enable the user can select a face on the graph. Used as preliminary step before splitting face and edges
S	Updates the x-y coordinates of the source vertex to the current cursor location
T	Updates the x-y coordinates of the target vertex to the current cursor location
	No Functionality Implemented
	No Functionality Implemented
	No Functionality Implemented
	No Functionality Implemented

Table 4.6: File menu Items description.

File Item	Description
Open File	Brings up a file selection panel, user can choose an existing graph file
Save File	Brings up a file save panel, the user can save a new file or replace an existing file
New	Clears the center display panel, ready for a new graph
Export to Xfig	Brings up file save panel, the file is saved in Xfig file format

Table 4.7: Options and Help menu Items description.

Options Item	Description
HalfEdge Display	When checked displays the half edges individually
Help Item	Description
Help Contents	Access to help information

#### 4.2.3 Program Submenu Description

The program's main GUI has three menu selections: File, Options, and Help. The File menu items enables the user to retrieve and open a previously saved file or to save the currently displayed network to a file, or to clear the display-screen. It also has an option

to export the network into Xfig format. A brief description of the File items is given in Table 4.6. The Options and Help items are described in Table 4.7. Figure 4.10 shows the GUI representation of the Options sub-menu items.

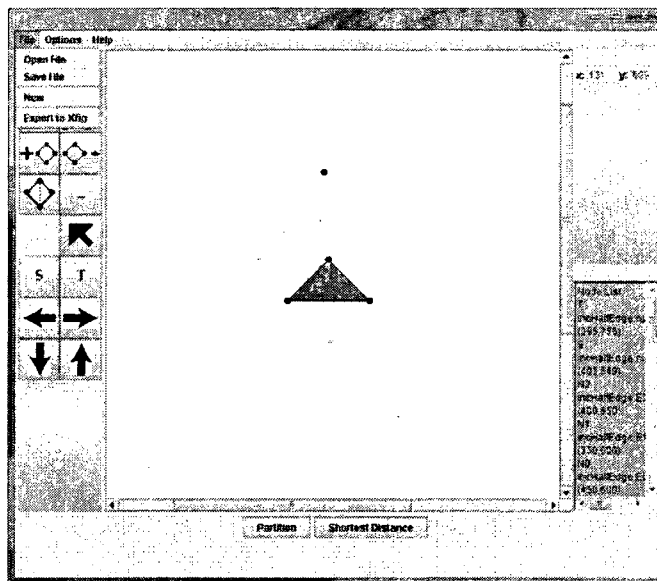


Figure 4.10: Planar Program File Options.

The secondary program GUI also has File and Options menus. The File menu has a single function that allows the user to save a network that has been partitioned. The Options menu lets the user enable/disable a step function. A detailed description of the sub menus is shown on Table 4.8. Figure 4.11 shows the GUI with the Options menu as presented to the user.

Table 4.8: File and Options menu Items description.

File Item	Description
Save File	Brings up a file save panel, the user can save the partitioned file
Options Item	Description
Enable Step Mode	Displays each step as program processes the vertices



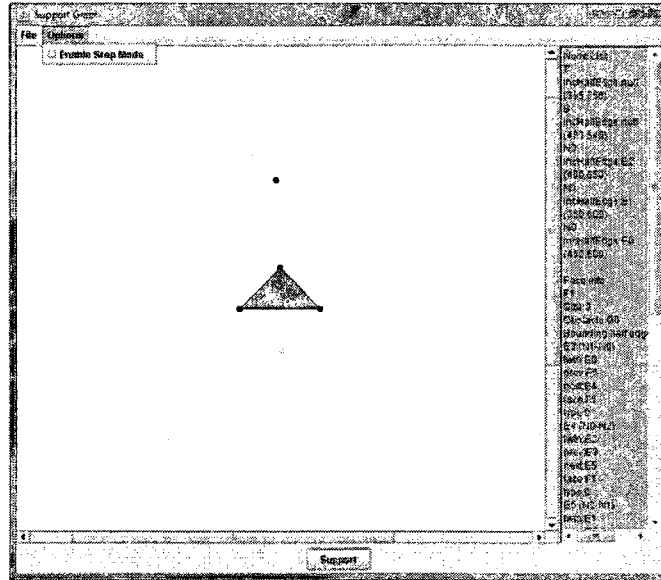


Figure 4.11: Planar Program Partition Options.

#### 4.2.4 SPM Implementation

The partitioning algorithm relies on maintaining a planar graph structure. The information is stored in four data structure implemented as java classes: Node, HalfEdge, Face, and Obstacle. They are used by the DCEL class which contains the support functions needed to create and modify a planar graph. The DCEL class has many support functions that include the following.

**public boolean addEdge(int x, int y)** - Adds a node with coordinates  $(x, y)$ . If necessary, it also adds the half-edges adjacent to the node.

**public void splitEdge(int x, int y)** - This function is used to split an existing edge into two parts. When an edge is split,  $(x, y)$  will be the coordinates of the new node used to split the edge. It is noted that when an edge is split, two half-edges are partitioned into four half-edges.

**public Face splitFace(HalfEdge edge1, HalfEdge edge2)** - This function is used to partition a currently selected face into two parts. The actual splitting is done by

connecting two non-consecutive vertices of the current face by a pair of half-edges.

`public boolean connectPaths(HalfEdge e1, HalfEdge e2)` - This function is used for adding an edge between two selected nodes. It is noted that when an edge is added it can either split a face or it can combine two holes. So if the added edge connects two nodes on the boundary of the same face then it splits that face. On the other hand if the nodes are on different holes then the connecting edge combines those holes into one.

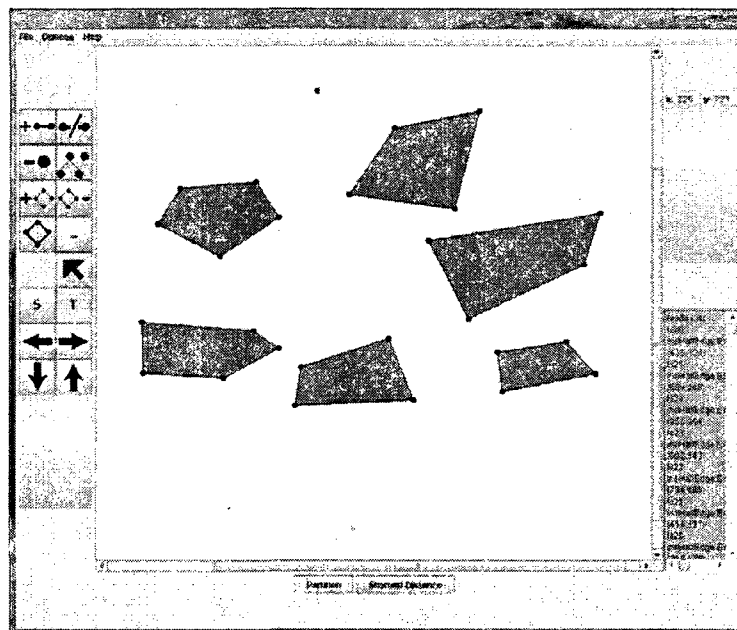


Figure 4.12: Graph G Before Partition.

Figure 4.12 shows an obstacle configuration, together with source vertex  $s$  and target vertex  $t$ , using the implemented functions of the DCEL data structure. When the partitioning of the free-space is completed by adding the connecting edges and the bisector hyperbola branches, we obtain the network shown in Figure 4.13. Now it is very convenient to compute the shortest path from the source vertex  $s$  to any query target vertex  $t$ . All the user has to do is to pick the target vertex  $t$  with a mouse-click and the program constructs the shortest path from  $s$  to  $t$ . One example of the shortest path is shown in

Figure 4.14.

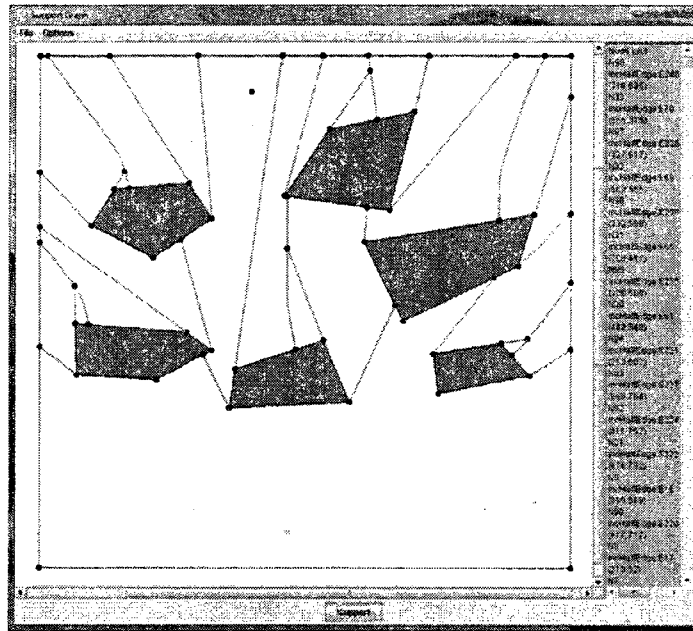


Figure 4.13: Graph G Partitioned into Regions.

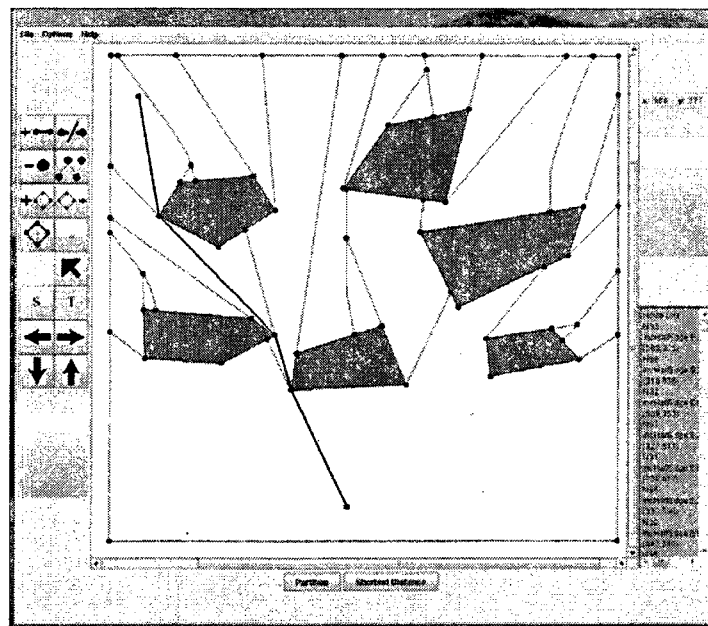


Figure 4.14: Shortest Path from s to t.

## CHAPTER 5

### CONCLUSION

In this thesis we presented an algorithm for computing Turn-Constrained  $k$  node-Disjoint Paths connecting two vertices in a geometric network. The time complexity for the algorithm is  $O(k|E|\log n)$ , where  $|E|$  is the number of edges in the network and  $n$  is the number of vertices. This algorithm is developed by extending the angle constrained path computation algorithm and disjoint path-pair algorithm reported in [1] and [8], respectively. The turn-angle constrained algorithm developed by Suurballe and Tarjan [13] is efficient theoretically but very difficult to implement due to the use of complicated data structures. Our algorithm combines the simpler disjoint path planning algorithm given in [8] with the graph transformation technique in [1] to obtain an algorithm that is simple for implementation.

We presented an implementation of the proposed Turn-Constrained  $k$  node disjoint path algorithm, done in the Java programming language. The prototype of the implementation has a graphical user interface GUI, that helps the user to compute  $k$ -disjoint paths by varying several parameters. The user can generate, modify, edit, save, and retrieve the network by dragging, moving and clicking the mouse buttons. We executed the implemented program on several networks. The generated solutions show that the implementation is indeed producing short-length paths that are node disjoint and without sharp turns.

The second problem we presented in this thesis is the construction of the shortest path map (SPM), which can be used for computing the shortest path from a fixed source vertex point to several query target points. We present a generalization of the standard shortest path map called the turn-constrained shortest path map. The turn-constrained

shortest path map can be used for constructing shortest path from a fixed source vertex  $s$  to varying query vertex  $q$  such that the generated paths do not have sharp turns. The presented algorithm is based on the repeated construction of the visibility polygon from the front nodes. The presented algorithm can be implemented in a straight forward manner. In fact, we presented an implementation of a prototype program for the standard shortest path map. The implementation of the constrained version is not complete but is in progress.

Several extensions of the proposed algorithms can be made in the future. The turn-constrained disjoint path algorithm presented in this thesis does produce very short length paths. But we have not been able to prove that the path pair are of shortest total length. It would be interesting to settle this issue.

The constrained shortest path map algorithm presented in this thesis can be used only in the presence of polygonal obstacles in two dimensions. A natural extension would be to look for the construction of shortest path maps in three dimensions. Since the problem of constructing shortest path in three dimensions is known to be intractable [2], the corresponding shortest path map construction problem in three dimensions should be very difficult. As a first step in this direction we plan to explore the construction of shortest path map in terrain surface which is generally viewed as two and half dimensions.

## BIBLIOGRAPHY

- [1] Ali Boroujerdi, Jeffrey Uhlmann, *An efficient algorithm for computing least cost paths with turn constraints*, Information Processing Letters 67 (1998) 317 - 321
- [2] John Canny, John Reif, *New Lower Bound Techniques for Robot Motion Planning Problems*, IEEE Proceedings of the 28th Annual Symposium on Foundations of Computer Science, (1987) pp 49 - 60
- [3] T. Cormen, C. Leiserson, R. Rivestam C. Stein, *Introduction to Algorithms*, MIT Press and McGraw-Hill, (2001)
- [4] E. W. Dijkstra, *A note on Two Problems in Connection with Graphs*, Numer. Math, 1 (1959) pp 269-271
- [5] Jonh Hershberger, Subhash Suri, *An optimal Algorithm for Euclidean Shortest Path in the Plane*, SIAM J. Comput. Vol 28 No 6 (1999) pp 2215-2256
- [6] J, Krozel, C. Lee, J. S. B. Mitchell, *Turn-Constrained Route Planning for Avoiding Hazardous Weather*, Air Traffic Control quarterly Vol 14(2) (2006) pp 159-182
- [7] Lee D. T , Preparata F. P., *Euclidean Shortest Path in the Presence of Rectilinear Barriers*, Networks Vol. 14 (1984) pp 393 - 410
- [8] Daniel Mazzella, *Disjoint Path in Geometric Graphs* MS Thesis, School of Computer Science Univ. of Nevada Las Vegas, (2006)
- [9] Joseph S. B. Mitchell, Gunter Rote, Gerhard Woeginger *Minimum-link path among obstacles in the plane*, Algorithmica, 6 (1992) pp 431-459
- [10] J. O'Rourke, *Computational Geometry in C*, Cambridge UniversityPress 2 (1998)

- [11] James A. Storer, John H. Reif, *Shortest Path in a the Plane with Polygonal Obstacles*, Journal of ACM vol 41, No 5, September (1984) pp 983 - 1012
- [12] S. Suri, J. O'rourke, *Worst-case optimal algorithms for constructing visibility polygons with holes*, Proceedings of the second annual symposium on Computational Geometry, (1986) pp 14 - 23
- [13] J. W. Suurballe, R. E. Tarjan, *A quick Method for Finding Shortest Pairs of Disjoint Paths*, Networks 14 (1984) pp 325-336

VITA

Graduate College  
University of Nevada, Las Vegas

Victor M. Roman

Local Address:

Las Vegas, NV

Degrees:

Bachelors of Science in Electronic Engineering, 1984  
Northrop University

Bachelors of Science in Computer Science, 2006  
University of Nevada, Las Vegas

Thesis Title: Turn Constrained Path Planning Problems

Thesis Examination Committee:

Chairperson, Dr. Laxmi Gewali Ph. D.

Committee Member, Dr. Jan B. Pedersen, Ph. D.

Committee Member, Dr. John Minor Ph. D.

Graduate Faculty Representative, Dr. Henry Selvaraj, Ph. D.